SDF-1 secreted by mesenchymal stem cells promotes the migration of endothelial progenitor cells via PI3K/Akt pathway

Xiaoyi Wang
Zhengzhou University School of Medicine First Affiliated Hospital
Huijiao Jiang
Medical College of Shihezi University
Lijiao Guo
Medical college of Shihezi University
Sibo Wang
Medical College of Shihezi University
Wenzhe Cheng
Medical College of Shihezi University
Longfei Wan
Medical College of Shihezi University
Zhongzhou Zhang
Medical College of Shihezi University
Lihang Xing
Medical College of Shihezi University
Qing Zhou
Medical College of Shihezi University
Xiongfeng Yang
Medical College of Shihezi University
Huanhuan Han
Medical College of Shihezi University
Xueling Chen
Medical college of Shihezi University
Xiangwei Wu (wxwshz@126.com)
Shihezi University School of Medicine https://orcid.org/0000-0002-3897-6629

Research

Keywords: MSCs, EPCs, Combination cell therapy, Mouse model of hind limb ischemia, SDF-1

Posted Date: March 5th, 2020

DOI: https://doi.org/10.21203/rs.3.rs-16131/v1

Abstract

Background: Cell-based therapeutics bring great hope in areas of unmet medical needs. Mesenchymal stem cells (MSCs) has been suggested to facilitate neovascularization mainly by paracrine action, and endothelial progenitor cells (EPCs) can differentiate into mature endothelial cells. Studies have demonstrated that a combination cell therapy that includes MSCs and EPCs has a favorable effect on ischemic limbs. However, the mechanism of combination cell therapy remains unclear. Herein, we investigate whether stromal cell-derived factor (SDF)-1 secreted by MSCs contributes to. Furthermore, we examined whether SDF-1 affects EPC migration via Phosphoinositide 3-Kinases (PI3K)/protein kinase B (termed as Akt) signaling pathway.

Methods: First, intramuscular MSC injections were supplemented with intravenous EPC injections in the mouse model of hind limb ischemia. The incorporation of Qdot® 525 labeled-EPC into the vasculature and capillary density was evaluated by CD31 immunohistochemistry and immunofluorescence, respectively. Then, the concentration of SDF-1 secreted by MSCs was detected via quantitative immunoassay. Flow cytometry was performed to quantify CXC chemokine receptor (CXCR) 4-positive EPCs. The effect of MSCs on EPC migration was measured by a transwell system and a tube-like structure formation on Matrigel. The SDF-1 antagonist AMD3100 and the PI3K inhibitor wortmannin were separately used to determine the participation of CXCR4 and PI3K into EPC migration. Finally, western blot assay was performed to detect the effect of SDF-1 secreted by MSCs on Akt phosphorylation in EPCs.

Results: The combination delivery of MSCs and EPCs via a “dual-administration” approach enhanced the incorporation of EPCs into the vasculature and increased the capillary density in mouse ischemic hind limb. The SDF-1 concentration secreted by MSCs was 2.61 ng/ml after 48 h. CXCR4-positive EPCs increased after incubation with MSC-conditioned medium (CM). MSCs contributed to EPC migration and tube-like structure formation, both of which were suppressed by AMD3100 and wortmannin. Phospho-Akt induced by MSC-CM was attenuated when EPCs were pretreated with AMD3100 and wortmannin.

Conclusions: The paracrine action of MSCs contributes to EPC migration. Furthermore, SDF-1 secreted by MSCs induces EPC migration. The mechanism of this migration is related to the activation of the Akt pathway

Introduction

Organisms require blood vessels to carry oxygen and nutrients for proper developmental and physiological functioning; however, abnormalities in this process may lead to disease development or progression. Tissue ischemia, which is characterized as an insufficient supply of oxygen and nutrients, impairs bodily functions and can even be life-threatening [1]. Naturally, neovascularization is required to maintain the integrity and function of ischemic tissues.

Currently, therapeutic neovascularization based on stem cells is under intense investigation. A combination cell therapy that includes EPCs and MSCs improves perfusion in patients with severe ischemic limbs [2–4]. However, the underlying mechanisms are poorly understood. A number of researchers have focused on SDF-1 and its receptor CXCR4 as critical regulators of stem cell recruitment [5, 6]. The delivery of SDF-1 contributes to ischemic neovascularization in vivo by augmenting EPC recruitment to ischemic tissues [7, 8]. Furthermore, SDF-1 mediates cell migration through the activation of the PI3K/AKT pathway [9]. MSCs secrete a vast array of chemoattractants, such as SDF-1, vascular endothelial growth factor, platelet-derived growth factor, hepatocyte growth factor, insulin-like growth factor-1, fibroblast growth factor, and hypoxia inducible factor-1α [10]. Studies suggest that the paracrine property of MSCs plays a greater role in therapeutic angiogenesis than their transdifferentiation or cell infusion [11, 12]. In view of the reasons stated above, we speculate that Akt protein is phosphorylated when SDF-1 secreted by MSCs engages the corresponding receptors CXCR4 on EPC surface, which in turn induces EPC migration.

Herein, we investigated whether a combination cell therapy that includes EPCs and MSCs improves perfusion in the mouse model of hind limb ischemia. We performed in vitro experiments to explore the potential molecular mechanisms involved in EPC migration. An excellent understanding of the mechanisms involved in the effect of cytokines secreted by MSCs on EPC migration will contribute to maximizing the local concentration of EPCs in the ischemic area and increase cell invasion. This information will provide insights into effective therapeutic approaches for cellular transplantation.

Materials And Methods

Mice

All animal experiments were performed in accordance with the Xinjiang Medical University Guide for Laboratory Animals. C57BL/6 mice that respectively were 1–2 (15–25 g) and 6–7 (25–30 g) months old were obtained from the Laboratory Animal Center of Xinjiang Medical University (Urumqi, China). Mice were maintained under a 12 h light/dark cycle in a constant temperature and humidity environment, food and water were available ad libitum. All of the experimental procedures were approved by the Shihezi University Ethics Committee (Shihezi, China).

Cell Isolation and Culture

MSCs and EPCs derived from murine bone marrow were simultaneously isolated as previously described [13]. MSCs were cultured in complete Dulbecco's modified Eagle's medium (DMEM) that consisted of low-glucose DMEM (Gibco; Thermo Fisher Scientific, Waltham, MA, USA), 10% fetal bovine serum (FBS; Hyclone, GE Healthcare Life Sciences, Logan, UT, USA), 100 U/ml penicillin, and 100 U/ml streptomycin (both from Sigma-Aldrich; Merck KGaA, Darmstadt, Germany). EPCs were cultured in endothelial growth medium (EGM) that contained endothelial cell basal medium-2, EGM™-2 MV SingleQuots™ (both from Lonza Group, Basel, Switzerland), 100 U/ml penicillin, and 100 U/ml streptomycin. Both were maintained

at 37 °C in a humidified 5% CO_2 incubator. When the cells reached 80–90% confluence, the cultures were harvested using StemPro Accutase (Gibco; Thermo Fisher Scientific).

Unilateral Hind Limb Ischemia (HLI) Model and Cell Transplantation

The femoral arteries of 6-month-old (30–35 g) male mice were ligated to induce left hind limb ischemia as described previously [14]. To track EPC incorporation at early time point after transplantation (on day 3), we seeded passage 3 cells in EGM in a 60 mm culture dish. When 80–90% confluence was reached, the cells were labeled using the Qtracker® 525 Cell Labeling Kit (Life technology, Carlsbad, CA, USA) according to the manufacturer's protocol. At 24 h after operation, the mice with ischemic limbs were randomly allocated into four groups as follows: phosphate-buffered saline (PBS) group; MSC (1×10^6) group; Qdot® 525 labeled-EPCs (1×10^6) group; and a combination of MSCs (1×10^6) and Qdot® 525 labeled-EPCs (1×10^6) group. Cells or PBS were administrated as above. After 3 days, the adductor muscles of ischemic and healthy limbs were immediately harvested for frozen section samples.

We also investigated the combination effect of MSCs and EPCs on neovascularization at late time point after transplantation (on day 14). At 24 h after operation, the mice were randomly allocated into four groups that received the following injections: PBS; MSCs (1×10^6); EPCs (1×10^6); or a combination of MSCs (1×10^6) and EPCs (1×10^6). MSCs suspended in 50 μl of PBS or PBS alone were infused to the gracilis muscles at four sites. Then, EPCs suspended in 20 μl of PBS or PBS alone were injected via the tail vein. After 14 days, the adductor muscles of ischemic and healthy limbs were harvested for paraffin section samples.

Histological Assessment of Transplanted Mice

For frozen section samples, tissues were embedded in OCT compound and snap frozen in liquid nitrogen. Frozen sections with a thickness of 8 μm were mounted on silane-coated glass slides and air-dried for 1 h. The section samples were then washed for 5 min thrice with PBS and blocked with normal goat serum (Solarbio, Beijing, China) for 20 min at room temperature (RT). Subsequently, the sections were stained with rabbit antibody against mouse CD31 (1:100; Cell Signaling Technology, Danvers, MA, USA) overnight at 4 °C. After three washes in PBS for a total of 30 min, a secondary TRITC-conjugated goat anti-rabbit IgG antibody (1:50; ZSGB-BIO, Beijing, China) was added for 30 min at RT. Any excess liquid was removed from the specimen, and one drop of the mounting reagent (glycerinum: PBS = 9:1) was applied (Thermo Fisher Scientific) to the specimens. Photographs were taken using a Zeiss LSM 510 META laser confocal microscope (Zeiss, Germany).

For paraffin section samples, tissues were fixed, dehydrated, and paraffin embedded. Paraffin sections with a thickness of 5 μm were prepared. Vascular density was determined by quantifying the CD31-positive vessels/mm^2 present in the peri-infarct region. The sections were incubated with primary rabbit anti-mouse CD31 (1:200; Abcam) and then with secondary horseradish peroxidase (HRP)-conjugated goat anti-rabbit antibody (1:10000; Abcam). After rinsing with PBS thrice, a DAB working solution was

added for 5 min. The sections were counterstained with hematoxylin for 10 s and mounted with neutral balsam. Photographs were taken using an inverted microscope (Olympus, Japan). CD31-positive staining was measured in two sections of four distinct views of each specimen by using the Image-Pro Plus 6.0 software.

Migration Assays

To investigate the effect of SDF-1 secreted by MSCs on EPC migration, we performed the assay using the transwell assembly (Corning) with 6.5 mm diameter inserts (8 μm pore size) as described previously [15]. Briefly, EPCs were pretreated with 50 ng/ml AMD3100 for 2 h [7] and 0.1 μM wortmannin for 1 h [16]. AMD3100 is a highly selective antagonist of SDF-1 that binds to its receptor, CXCR4. By comparison, wortmannin is a PI3K inhibitor. Non-pretreated EPCs and pretreated EPCs (1×10^5) were harvested and suspended in 100 μl of EBM-2 supplemented with 2% FBS and then reseeded in the upper compartment. MSCs (5×10^4) were suspended in 600 μl EBM-2 supplemented with 2% FBS and replated in the lower compartment of the transwell chamber. After incubation at 37 °C for 18 h, the cells on the filters were stained with 0.1% crystal violet. Thereafter, the filters were washed with 33% acetic acid, and the OD_{570} nm value of the eluate was detected using a spectrophotometer (Thermo Fisher Scientific).

Preparation of MSC-conditioned Media (MSC-CM)

MSCs were seeded in DMEM supplemented with 10% FBS until 90% confluence. After washing the cells with PBS, the medium was changed into EBM supplemented with 1% BSA and conditioned at 37 °C and 5% CO_2. After 24 and 48 h, the medium was collected and centrifuged at 300 g for 10 min to remove cell debris and then filtered (0.22 μm pore size; Merck Millipore, Billerica, MA, USA). The control medium comprised EBM and 1% BSA in the absence of cell procedure.

Flow Cytometry Analysis of CXCR4 Expression on EPCs Induced by MSC-CM

We investigated whether SDF-1 secreted by MSCs affects CXCR4 expression in EPCs. First, quantitative immunoassay was used to assess the ability of MSCs to produce SDF-1 according to the manufacturer's protocol (Elabscience, Wuhan, China). The MSC-CM obtained above was detected. Data were acquired using a spectrophotometer, and measurement wavelength was 450 nm.

CXCR4 expression in EPCs was measured via flow cytometry. EPCs were cultured with EGM until 90% confluence. After serum-free starvation overnight, EPCs were divided into four groups and cultured with EBM + 2% FBS, MSC-CM + 2% FBS for 24 h, MSC-CM + 2% FBS for 48 h, and MSC-CM + 2% FBS for 72 h. Then, EPCs were harvested and incubated with rabbit anti-mouse CXCR4 antibody (Abcam) for 30 min at RT, washed with PBS thrice, and incubated with TRITC-conjugated goat anti-rabbit IgG at 4 °C in the dark. Data were acquired using a flow cytometer (Becton Dickinson, USA).

Tube-like Structure Formation Assays

The tubule formation assays were performed with a thick Matrigel (BD Biosciences) according to the manufacturer's instruction. Briefly, a pre-cooled 48-well plate was coated with the Matrigel, which was melted into liquid at 4 °C overnight. The plate was placed at 37 °C and 5% CO_2 for 45 min to allow polymerization of the Matrigel. Meanwhile, EPCs were pretreated with 50 ng/ml AMD3100 for 2 h and 0.1 μM wortmannin for 1 h. The nonpretreated EPCs and pretreated EPCs (2×10^4) were suspended in 350 μl of MSC-CM or EBM supplemented with 2% FBS and then inoculated on top of the Matrigel. After incubating for 6–8 h at 37 °C and 5% CO_2, all wells were photographed (× 5 amplification) using an inverted microscope (Zeiss). Tubule formation was quantified with the Angiogenesis analyzer from Image-Pro Plus 6.0.

Western Blot Assays

To investigate the migration signaling, we pre-incubated EPCs with 50 ng/ml AMD3100 for 2 h and 0.1 μM wortmannin for 1 h. The EPCs were then incubated for 30 min with MSC-CM + 5% FBS. Cells were harvested for immunoblotting of phospho-Akt and total Akt. Extracts were prepared using a lysis buffer solution (RIPA:PMSF:protein phosphatase inhibitor = 100:1:1; Solarbio). Proteins were measured using the Pierce™ BCA protein assay kit (Pierce; Thermo Scientific) with BSA as a standard. Equal amounts of proteins (20 μg) were separated in 10% sodium dodecyl sulfate-polyacrylamide gel electrophoresis and transferred to nitrocellulose membranes (Amersham Biosciences). The membranes were then blocked with 5% nonfat dried milk in Tween phosphate-buffered saline (T-PBS) and probed with rabbit polyclonal anti-phospho-Akt (1:2000; Cell Signaling Technology) and total Akt (1:2000; Cell Signaling Technology) antibody overnight at 4 °C. After incubation with primary antibody, blots were washed thrice in T-PBS and incubated for 1 h with anti-rabbit HRP-conjugated IgG (1:10,000; Abcam). The protein bands were detected by Odyssey CLx system (Gene Company Limited, Hong Kong, China), and the intensities of the immunoblot bands were quantified using the Odyssey CLx Image Studio 3.1. Immunoblots were re-probed with rabbit anti-mouse β-actin (Abcam) for normalization. After digitization, band intensities were evaluated with GraphPad Prism 5 (GraphPad Software, CA, USA) and presented as a ratio of phosphated Akt protein intensity to β-actin intensity and to Akt intensity.

Statistical Analysis

All values were expressed as mean ± standard deviation of the mean. One-way ANOVA was used to compare the difference between groups. Statistical analysis was performed using GraphPad Prism 6.0, and p value < 0.05 was considered statistically significant.

Results

Contribution of MSCs to EPC Incorporation into Ischemic Hind Limb Neovasculature

To study the effect of MSCs on recruitment of EPCs from the systemic circulation, we measured the incorporation of injected EPCs into the microvasculature in the ischemic hind limb. Transplanted EPCs labeled with Q-tracker were identified in tissue sections by green fluorescence, whereas the native mouse

vasculature stained by anti-CD31 antibody was identified by red fluorescence in the same tissue sections. Three days after cell administration, the incorporation of EPCs into vasculature increased in the combined group compared with that in the EPC group (Fig. 1).

Local Delivery of MSCs Increase Vascular Ratio per Area

Angiogenesis promoted by MSCs results from the paracrine effect; hence, we evaluated its beneficial effect with the combined cell therapy. The nuclei of muscle cells were on the edge, and they moved inward when muscle cells degenerated. At 14 days after cell delivery, hematoxylin and eosin (HE) staining showed that a small number of nuclei were located in the center of muscle cells in the combination group of MSCs and EPCs in contrast to the PBS and EPC groups.

The vascular ratio per area was represented by CD31-positive staining. It was significantly higher in the combined group than in the PBS and MSC groups. Although the vascular ratio increased in the EPC group, no statistically significant difference was observed compared with the combined group (Fig. 2).

In Vitro Results

SDF-1 Production by MSCs and CXCR4 Expression by EPCs

We performed ELISA assay with MSC-CM. After 24 and 48 h, SDF-1 secreted by MSCs was 0.62 and 2.61 ng/ml, respectively.

To assess the potential effects of MSC-CM on CXCR4 expression, we cultured EPCs in MSC-CM with 5% FBS for 24, 48, and 72 h. The cells were recovered, and CXCR4 was measured via flow cytometry. Results showed that the expression of CXCR4-positive EPCs was 50.3%, 67.6%, and 51.9% after 24, 48, and 72 h, respectively. By contrast, the expression of CXCR4-positive EPCs was 27.7% when cultured in EBM with 5% FBS. Statistically, the protein level of CXCR4 in EPCs significantly increased after incubation with MSC-CM.

(A) Levels of SDF-1 secreted by MSCs at 24 and 48 h. (B) Representative flow cytometric analysis of CXCR4 expression (blank space) from EPCs; red space represents isotype controls. (C) Quantification analysis of CXCR4-positive EPCs induced by MSC-CM. Each experiment was repeated thrice. ***$p < 0.001$.

Effect of SDF-1 Secreted by MSCs on EPC Migration

EPC migration is a critical step in neovascularization. Transwell migration assay revealed that EPCs, which migrated to the lower surface of the inserts, significantly increased in the MSC-CM group compared with the EBM group. We examined the mechanism of SDF-1 secreted by MSCs on EPC migration with AMD3100 and wortmannin. Notably, the pre-incubation of AMD3100 or wortmannin resulted in significantly less EPC migration than that seen in the MSC-CM group (Figs. 4A and B). The results demonstrated that blockade of CXCR4 remarkably suppressed EPC migration induced by MSCs similar to the blockade of PI3K.

Effect of SDF-1 in MSC-CM on Tube-like Structure Formation of EPCs

Cell migration was also included in the process of tube-like structure formation. Compared with EBM, EPCs migrated, assembled, and formed complete tube-like structures under MSC-CM induction. The pre-incubation of AMD3100 or wortmannin resulted in incomplete tubule formation than that seen in no pre-incubation group containing MSC-CM. These structures were quantified with total mesh area and total segment length. The data indicated that the number of total mesh area and total segment length significantly decreased with AMD3100 or wortmannin pre-incubation. The blockade of CXCR4 has been suggested to suppress the formation of a tube-like structure similar to the blockade of PI3K.

(A) Tube-like structures were formed by EPCs under the indicated conditions (n = 3). Scale bar, 200 μm. (B) Quantification of total mesh area and total segment length in the tube-like structure. The experiment was repeated thrice. $^{**}p < 0.01$, $^{***}p < 0.001$.

Effect of SDF-1 in MSC-CM onAkt Phosphorylation in EPCs

To investigate whether SDF-1 in MSC-CM affects Akt phosphorylation, we evaluated Akt Ser473 phosphorylation in EPCs stimulated with MSC-CM for 30 min. Western blot analysis revealed that the level of phospho-Akt remarkably increased, and the increase was significantly suppressed by AMD3100 or wortmannin (Fig. 6).

Fig 6. Role of the Akt pathway in MSC-secreted SDF-1 induction of EPC migration. (A) Expression of Akt protein and Akt phosphorylation levels in EPCs cultured for 30 min in the EBM, MSC-CM, MSC-CM + AMD3100, and MSC-CM + wortmannin groups. (B) Bar graphs show the ratio of the densitometry measurement of phosphor-Akt to that of β-actin and to that of Akt. Data were obtained from three independent experiments. $^{*}p < 0.05$, $^{**}p < 0.01$, $^{***}p < 0.001$, NS: no significance.

Discussion

The therapeutic approach of combined MSCs and EPCs stems from the evidence that the process of angiogenesis may need more than one cytokine or cell type to optimize new vessel formation. EPCs might be fundamentally used to refer to populations of cells that are capable of differentiation into mature endothelial cells, with purported physiological roles in neovascularization [17]. Several clinical and preclinical studies have documented that administrated EPCs successfully augment neovascularization in multiple animal models of vascular injury [18, 19]. An important challenge for therapeutic neovascularization is the migration of a sufficient number of EPCs to the injury site to participate in neovascularization. EPCs cultured in vitro are distinguished into early and late EPCs depending on their time of appearance in culture [20]. In the present study, we used late EPCs to identify their integration into endothelium because early EPCs generate high levels of angiogenic cytokines, and late EPCs have the potential to form blood vessels [21].

MSCs are non-hemopoietic stromal cells, which are characterized by the multilineage differentiation potential, paracrine action, and low immunogenicity. MSCs make an important contribution to postnatal vasculogenesis, especially during tissue ischemia [22]. Mounting evidence shows that paracrine action probably underlie the vascular effects of MSCs [23–25]. Moreover, the conditioned medium of MSC cultures induces fibroblast, keratinocyte, and endothelial cell migration and promotes the formation of capillary-like structures by HUVECs [26].

In combined cell therapy, we critically consider the delivery methods of cells aside from the selection of cell types. To maximize the local concentration of EPCs in the ischemic area and increase cell invasion, we chose to implement a “dual-administration” approach, which was developed by Franz and Bartsch to treat patients with arterial occlusive disease [27–29]. In this approach of the present study, intramuscular MSC injections were supplemented with intravenous EPC injections in contrast to previous works in which the subjects received a mixture of MSCs and EPCs [30, 31]. The theoretical foundation of the design is that cytokines are the crucial stimulating factor for stem cell homing, and they build an attractive gradient, forming migratory route and guiding EPC migration to the region to be vascularized [32, 33]. To generate as many chemoattractants as possible, we envisioned that a vast array of chemoattractants secreted by intramuscular-administrated MSCs are locally deposited in ischemic muscle, attracting the homing of intravenous-administrated EPCs. Our results showed that Qdot® 525 labeled-EPCs in vasculature increased, and vessel numbers also increased when the combination of MSCs and EPCs was infused into the hind limb of ischemic mice. Thus, we conclude that chemoattractants secreted by MSCs promote EPC migration to the neovascularization sites.

We explored the molecular mechanism involved in EPC migration via in vitro experiments. Previous studies have suggested that SDF-1 induces EPC migration after binding to CXCR4, which is highly expressed on EPCs [34, 35]. In the present work, SDF-1 concentration increased in MSC culture supernatants of different time spans. In addition, the level of CXCR4 protein in EPCs increased after incubation in MSC-CM. The data indicated that SDF-1 produced by MSCs promotes CXCR4 expression in EPCs.

Akt, a multifunctional serine/threonine protein kinase, is the downstream of class I PI3K and various receptors. PI3K-Akt signaling pathway also has a crucial effect on multiple processes, including cell proliferation, cell survival, cell migration, activation of integrins, MMP, and angiogenesis. Using both chemical inhibitors to detect the role of PI3K/Akt signaling, we found that CXCR4 and PI3K participate in EPC migration. Furthermore, Akt phosphorylation results in cytoskeleton changes in many cells [36]. In the present study, Akt phosphorylation induced by MSC-CM was inhibited by both AMD3100 and wortmannin, indicating that phospho-Akt is the downstream of SDF-1/CXCR4/PI3K. Consistent with our results, Yu et al. revealed that SDF-1/CXCR4 mediates the migration of BMSCs toward heart MI through the activation of PI3K/Akt [37]. Dimova et al. reported that SDF-1 treatment of cardiac stem/progenitor cells increase Akt phosphorylation [38].

Conclusion

In a word, we argue that in combined cell therapy, MSCs facilitate the migration of circulating EPCs to neovascularization sites via the SDF-1/CXCR4/PI3K/Akt signaling pathway. Herein, we provided new insights into the mechanisms underlying the effects of combined cell therapy. These novel findings suggest that the modulation of the homing mechanism may be used as a therapeutic strategy to improve the efficacy of stem cell therapy [39].

Declarations

Acknowledgements

Not applicable.

Funding

This work was supported by grants from the National Natural Science Foundation of China (No. 81760570, No. 81760371, No. 81602810, No. 81703174) and the Project of Young and Middle-aged Scientific and Technological Innovation Leaders in Bingtuan (2018CB017).

Availability of data and materials

All data generated or analysed during this study are included in this published article.

Ethics approval and consent to participate

Animal experiments were approved by the Shihezi University Ethics Committee (Approval Number: A2017-008-01).

Authors' contributions

XWW and XC conceived and designed the experiments, and sourced for funding of the research. XYW wrote the manuscript. ZZ and HH cultured MSCs and EPCs, and critically revised the manuscript. XYW, HJ, LG, QZ performed the establishment of the mouse model of hind limb ischemia, immunohistochemistry and capillary density analysis. LW and LX prepared MSC-CM, performed flow cytometry and analysed the data. SW performed the migration assays and analysed the data. WC performed tube-like structure formation assays and analysed the data. XYW and XY performed western blot assays and analysed the data. All the authors read and approved the final version of the manuscript.

Competing interests

The authors declare that they have no competing interests.

Consent for publication

Not applicable.

Author details

1 Department of Pediatric Medicine, First Affiliated Hospital, School of Medicine, Zhengzhou University, No.1 Jianshe East Road, Zhengzhou, Henan 450052, People's Republic of China. 2 Laboratory of Translational Medicine, School of Medicine, Shihezi University, No.59 North 2 Road, Shihezi, Xinjiang 832002, People's Republic of China. 3 Department of General Surgery, First Affiliated Hospital, School of Medicine, Shihezi University, No.107 North 2 Road, Shihezi, Xinjiang 832008, People's Republic of China. 4 Department of Immunology, School of Medicine, Shihezi University, No.59 North 2 Road, Shihezi, Xinjiang 832002, People's Republic of China.

Abbreviations

Akt: protein kinase B; CM: conditioned medium; CXCR: CXC chemokine receptor; DMEM: Dulbecco's modified Eagle's medium; EGM: endothelial growth medium; EPCs: endothelial progenitor cells; FBS: fetal bovine serum; HE: hematoxylin and eosin; HLI: Hind Limb Ischemia; HRP: horseradish peroxidase; MSCs: mesenchymal stem cells; PI3K: phosphoinositide 3-kinases; RT: room temperature; SDF: stromal cell-derived factor; T-PBS: Tween phosphate-buffered saline

References

1.Thierry Couffinhal MS, LuP. Zheng, Marianne Kearney BW, Isner JM. Mouse Model of Angiogenesis. *Am J Pathol*. 1998;152:1667-79.

2.Lasala GP, Silva JA, Gardner PA, Minguell JJ. Combination stem cell therapy for the treatment of severe limb ischemia: safety and efficacy analysis. *Angiology*. 2010;61:551-6.

3.Lasala GP, Silva JA, Kusnick BA and Minguell JJ. Combination stem cell therapy for the treatment of medically refractory coronary ischemia: a Phase I study. *Cardiovasc Revasc Med*. 2011;12:29-34.

4.Lasala GP, Silva JA and Minguell JJ. Therapeutic angiogenesis in patients with severe limb ischemia by transplantation of a combination stem cell product. *J Thorac Cardiovasc Surg*. 2012;144:377-82.

5.Ghadge SK, Mühlstedt S, Özcelik C and Bader M. SDF-1α as a therapeutic stem cell homing factor in myocardial infarction. *Pharmacol Ther*. 2011;129:97-108.

6.Yu Q, Liu LZ, Lin J, Wang Y, Xuan XB, Guo Y, Hu SJ. SDF-1α/CXCR4 axis mediates the migration of mesenchymal stem cells to the hypoxic-ischemic brain lesion in a rat model. *Cell J*. 2015;16:440-7.

7.Yin Y, Zhao X, Fang Y, Yu S, Zhao J, Song M, Huang L. SDF-1α involved in mobilization and recruitment of endothelial progenitor cells after arterial injury in mice. *Cardiovasc Pathol*. 2010;19:218-27.

8.Tsai FC, Seki A, Yang HW, Hayer A, Carrasco S, Malmersjo S, Meyer T. A polarized Ca^{2+}, diacylglycerol and STIM1 signalling system regulates directed cell migration. *Nat Cell Biol*. 2014;16:133-44.

9.Liu X, Duan B, Cheng Z, Jia X, Mao L, Fu H, Che Y, Ou L, Liu L, Kong D. SDF-1/CXCR4 axis modulates bone marrow mesenchymal stem cell apoptosis, migration and cytokine secretion. *Protein Cell*. 2011;2:845-54.

10.Vanden Berg-Foels WS. In situ tissue regeneration: chemoattractants for endogenous stem cell recruitment. *Tissue Eng Part B Rev*. 2014;20:28-39.

11.Pankajakshan D, Agrawal DK. Mesenchymal stem cell paracrine factors in vascular repair and regeneration. *J Biomed Technol Res*. 2014;1:1-21.

12.Kwon HM, Hur SM, Park KY, Kim CK, Kim YM, Kim HS, Shin HC, Won MH, Ha KS, Kwon YG, Lee DH, Kim YM. Multiple paracrine factors secreted by mesenchymal stem cells contribute to angiogenesis. *Vascul Pharmacol*. 2014;63:19-28.

13.Wang X, Zhao Z, Zhang H, Hou J, Feng W, Zhang M, Guo J, Xia J, Ge Q, Chen X, Wu X. Simultaneous isolation of mesenchymal stem cells and endothelial progenitor cells derived from murine bone marrow. *Exp Ther Med*. 2018;16:5171-7.

14.Niiyama H, Huang NF, Rollins MD, Cooke JP. Murine model of hindlimb ischemia. *J Vis Exp*. 2009;(23), e1035:1-4.

15.Yamaguchi Ji, Kusano KF, Masuo O, Kawamoto A, Silver M, Murasawa S, Bosch-Marce M, Masuda H, Losordo DW, Isner JM, Asahara T. Stromal cell-derived factor-1 effects on ex vivo expanded endothelial progenitor cell recruitment for ischemic neovascularization. *Circulation*. 2003;107:1322-8.

16.Teranishi F, Takahashi N, Gao N, Akamo Y, Takeyama H, Manabe T, Okamoto T. Phosphoinositide 3-kinase inhibitor (wortmannin) inhibits pancreatic cancer cell motility and migration induced by hyaluronan in vitro and peritoneal metastasis in vivo. *Cancer Sci*. 2009;100:770-7.

17.Chong MSK, Ng WK, Chan JKY. Concise review: endothelial progenitor cells in regenerative medicine: applications and challenges. *Stem Cells Transl Med*. 2016;5:530-8.

18.Sun Y, Feng Y, Zhang C, Cheng X, Chen S, Ai Z, Zeng B. Beneficial effect of autologous transplantation of endothelial progenitor cells on steroid-induced femoral head osteonecrosis in rabbits. *Cell Transplant*. 2011;20:233-43.

19.Kawamoto A, Gwon HC, Iwaguro H, Yamaguchi J-i, Uchida S, Masuda H, Silver M, Ma H, Kearney M, Isner JM, Asahara T. Therapeutic potential of ex vivo expanded endothelial progenitor cells for myocardial ischemia. *Circulation*. 2001;103:634-7.

20.Medina RJ, Barber CL, Sabatier F, Dignat-George F, Melero-Martin JM, Khosrotehrani K, Ohneda O, Randi AM, Chan JKY, Yamaguchi T, Van Hinsbergh VWM, Yoder MC, Stitt AW. Endothelial progenitors: a consensus statement on nomenclature. *Stem Cells Transl Med*. 2017;6:1316-20.

21.Barsotti MC, Di Stefano R, Spontoni P, Chimenti D, Balbarini A. Role of endothelial progenitor cell mobilization after percutaneous angioplasty procedure. *Curr Pharm Des*. 2009;15:1107-22.

22.Ball SG, Shuttleworth CA, Kielty CM. Mesenchymal stem cells and neovascularization: role of platelet-derived growth factor receptors. *J Cell Mol Med*. 2007;11:1012-30.

23.Gulati R, Simari RD. Defining the potential for cell therapy for vascular disease using animal models. *Dis Model Mech*. 2009;2:130-7.

24.Gnecchi M, He HM, Liang Olin D, Melo Luis G, Morello F, Mu H, Noiseux N, Zhang LN, Pratt RE, Ingwall JS, Dzau VJ. Paracrine action accounts for marked protection of ischemic heart by Akt-modified mesenchymal stem cells. *Nat Med*. 2005;11:367-8.

25.Tang YL, Zhao Q, Qin X, Shen L, Cheng L, Ge J, Phillips MI. Paracrine action enhances the effects of autologous mesenchymal stem cell transplantation on vascular regeneration in rat model of myocardial infarction. *Ann Thorac Surg*. 2005;80:229-36.

26.Pereira AR, Mendes TF, Ministro A, Teixeira M, Filipe M, Santos JM, Barcia RN, Goyri-O'Neill J, Pinto F, Cruz PE, Cruz HJ, Santos SC. Therapeutic angiogenesis induced by human umbilical cord tissue-derived mesenchymal stromal cells in a murine model of hindlimb ischemia. *Stem Cell Res Ther*. 2016;7:145.

27.Franz RW, Parks A, Shah KJ, Hankins T, Hartman JF, Wright ML. Use of autologous bone marrow mononuclear cell implantation therapy as a limb salvage procedure in patients with severe peripheral arterial disease. *J Vasc Surg*. 2009;50:1378-90.

28.Bartsch T, Brehm M, Zeus T, Kogler G, Wernet P, Strauer BE. Transplantation of autologous mononuclear bone marrow stem cells in patients with peripheral arterial disease (the TAM-PAD study). *Clin Res Cardiol*. 2007;96:891-9.

29.Franz RW, Shah KJ, Pin RH, Hankins T, Hartman JF, Wright ML. Autologous bone marrow mononuclear cell implantation therapy is an effective limb salvage strategy for patients with severe peripheral arterial disease. *J Vasc Surg*. 2015;62:673-80.

30.Sanchez O, Bernabeu C, Mignon V, Planquette B, Gendron N, Guerin C, Lokajczyk A, Bacha N, Dizier B, Cras A, Goyard C, Rossi E, Smadja D. Co-injection of mesenchymal stem cells with endothelial progenitor cells accelerates muscle recovery in hind limb ischemia through an endoglin-dependent mechanism. *Thromb Haemost*. 2017;117:1908-18.

31.Traktuev DO, Prater DN, Merfeld-Clauss S, Sanjeevaiah AR, Saadatzadeh MR, Murphy M, Johnstone BH, Ingram DA, March KL. Robust functional vascular network formation in vivo by cooperation of adipose progenitor and endothelial cells. *Circ Res*. 2009;104:1410-20.

32.Schmidt A, Brixius K, Bloch W. Endothelial precursor cell migration during vasculogenesis. *Circ Res*. 2007;101:125-36.

33.Iwaguro H, Yamaguchi J-i, Kalka C, Murasawa S, Masuda H, Hayashi S-i, Silver M, Li T, Isner JM, Asahara T. Endothelial progenitor cell vascular endothelial growth factor gene transfer for vascular regeneration. *Circulation*. 2002;105:732-8.

34.Walter DH, Haendeler J, Reinhold J, Rochwalsky U, Seeger F, Honold J, Hoffmann J, Urbich C, Lehmann R, Arenzana-Seisdesdos F, Aicher A, Heeschen C, Fichtlscherer S, Zeiher AM, Dimmeler S. Impaired CXCR4 signaling contributes to the reduced neovascularization capacity of endothelial progenitor cells from patients with coronary artery disease. *Circ Res*. 2005;97:1142-51.

35.Wright LM, Maloney W, Yu X, Kindle L, Collin-Osdoby P, Osdoby P. Stromal cell-derived factor-1 binding to its chemokine receptor CXCR4 on precursor cells promotes the chemotactic recruitment, development and survival of human osteoclasts. *Bone*. 2005;36:840-53.

36.Chen J, Crawford R, Chen C, Xiao Y. The key regulatory roles of the PI3K/Akt signaling pathway in the functionalities of mesenchymal stem cells and applications in tissue regeneration. *Tissue Eng Part B Rev*. 2013;19:516-28.

37.Yu J, Li M, Qu Z, Yan D, Li D, Ruan Q. SDF-1/CXCR4-mediated migration of transplanted bone marrow stromal cells towards areas of heart myocardial infarction via activation of PI3K/Akt. *J Cardiovasc Pharmacol*. 2010;55:496-505.

38.Dimova N, Wysoczynski M, Rokosh G. Stromal cell derived factor-1a promotes c-kit^{+} cardiac stem/progenitor cell quiescence through casein kinase 1α and GSK3β. *Stem Cells* 2014;32:487–99.

39.Hur J, Yoon C, Lee C, Kim T, Oh I, Park K, Kim J, Lee H, Kang H, Chae I, Oh B, Park Y, Kim H. Akt is a key modulator of endothelial progenitor cell trafficking in ischemic muscle. *Stem Cells*. 2007;25:1769-78.

Figures

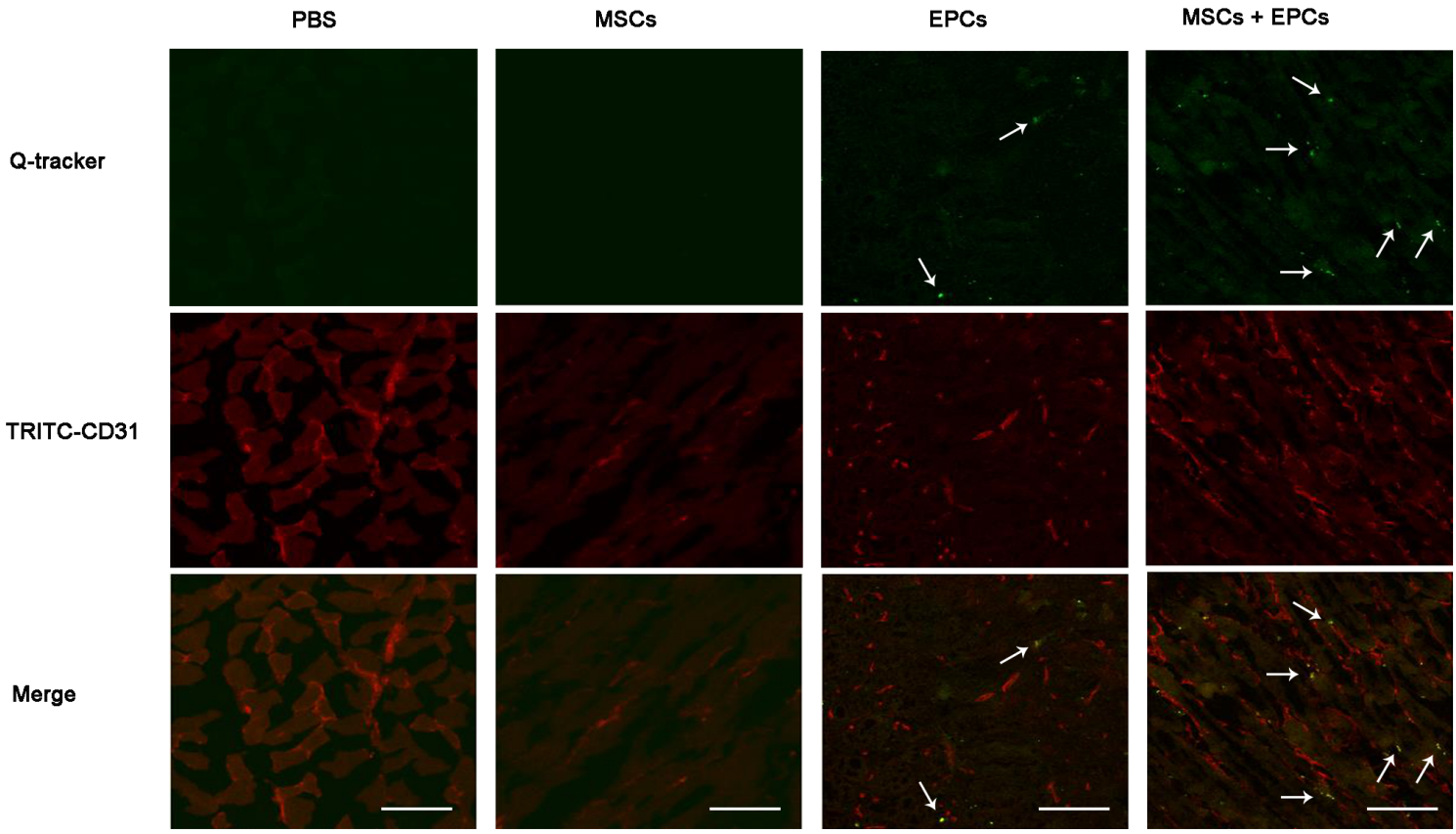

Figure 1

Representative photomicrographs of EPC incorporation into neovasculature sites in vivo. The top, middle, and bottom panels showed Q-tracker-labeled EPCs (green, indicated by arrows) between the skeletal myocytes, CD31-positive vasculature (red), and EPC incorporation into vasculature (yellow, indicated by arrows), for 3 days after administration (n = 3). Scale bar, 100 μm.

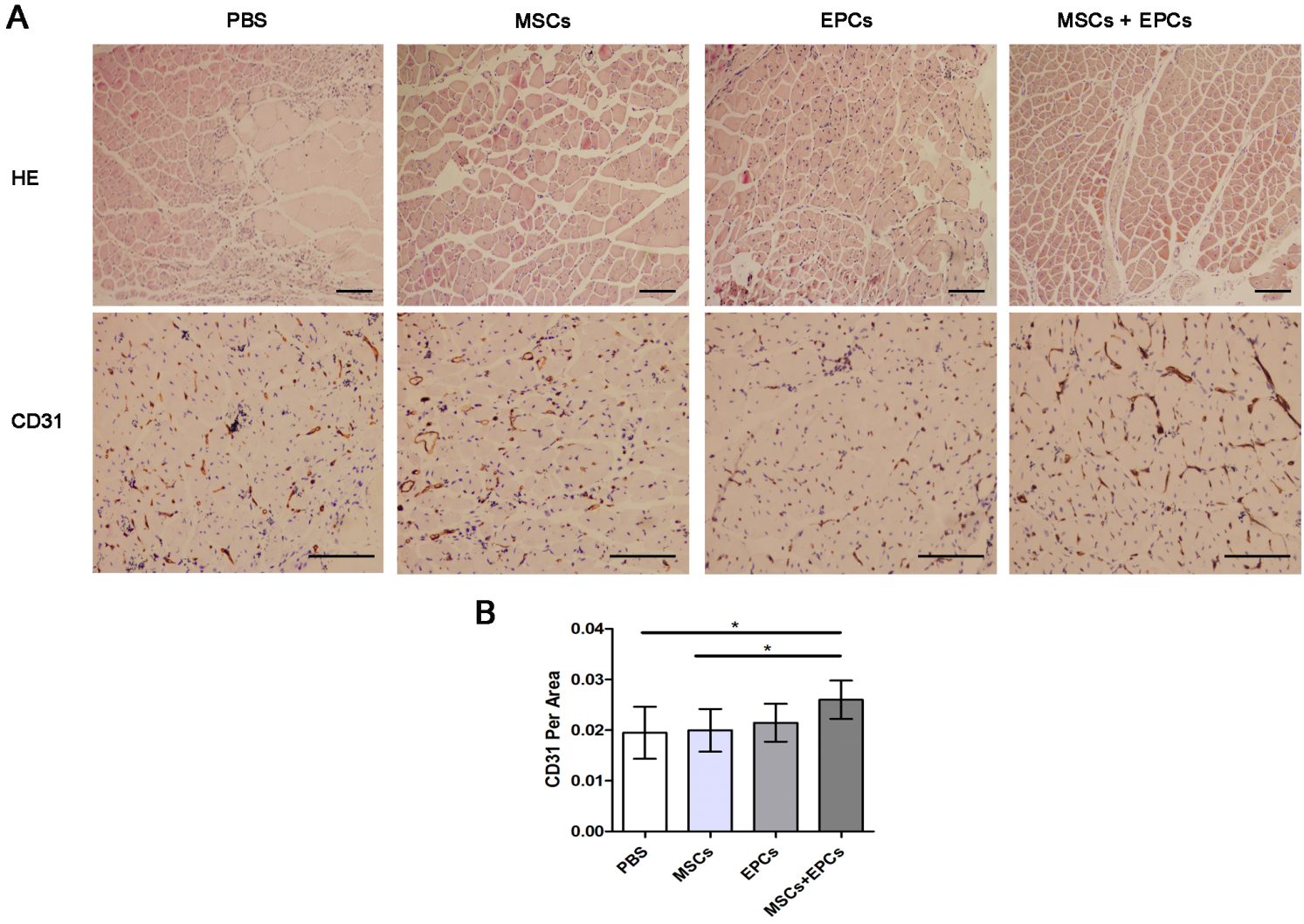

Figure 2

Histological analysis of adductor muscles. (A) Representative sections from PBS and cell-treated ischemic adductor muscles at 14 days post-HLI. Skeletal muscle cells and capillaries were identified by HE staining in top panels and CD31 immunohistochemistry in bottom panels, respectively (n = 3). Scale bar, 100 μm. (B) Quantification analysis of vascular ratio per area. *p < 0.05.

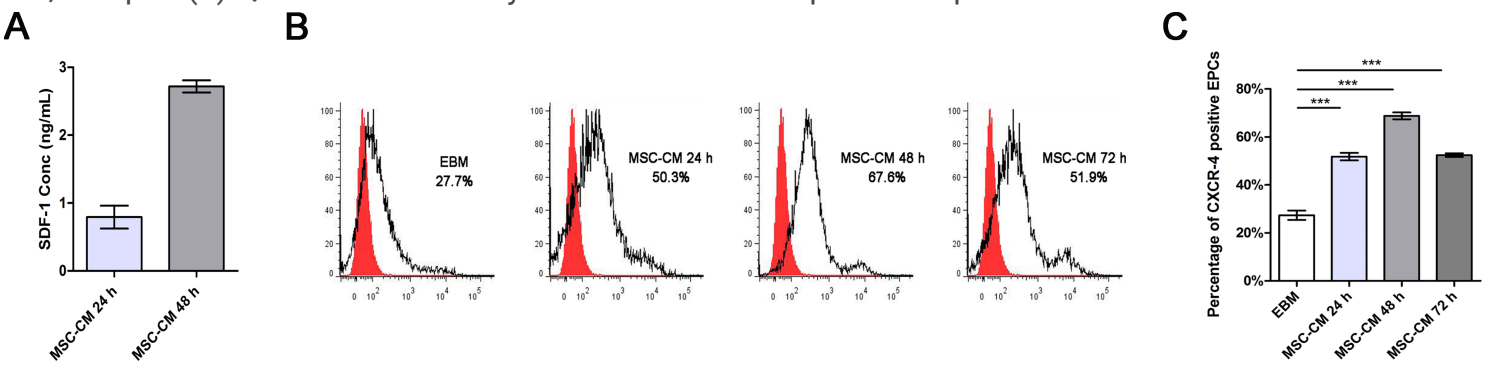

Figure 3

Level of SDF-1 in MSC-CM and CXCR4-positive EPCs. (A) Levels of SDF-1 secreted by MSCs at 24 and 48 h. (B) Representative flow cytometric analysis of CXCR4 expression (blank space) from EPCs; red space represents isotype controls. (C) Quantification analysis of CXCR4-positive EPCs induced by MSC-CM. Each experiment was repeated thrice. ***p < 0.001.

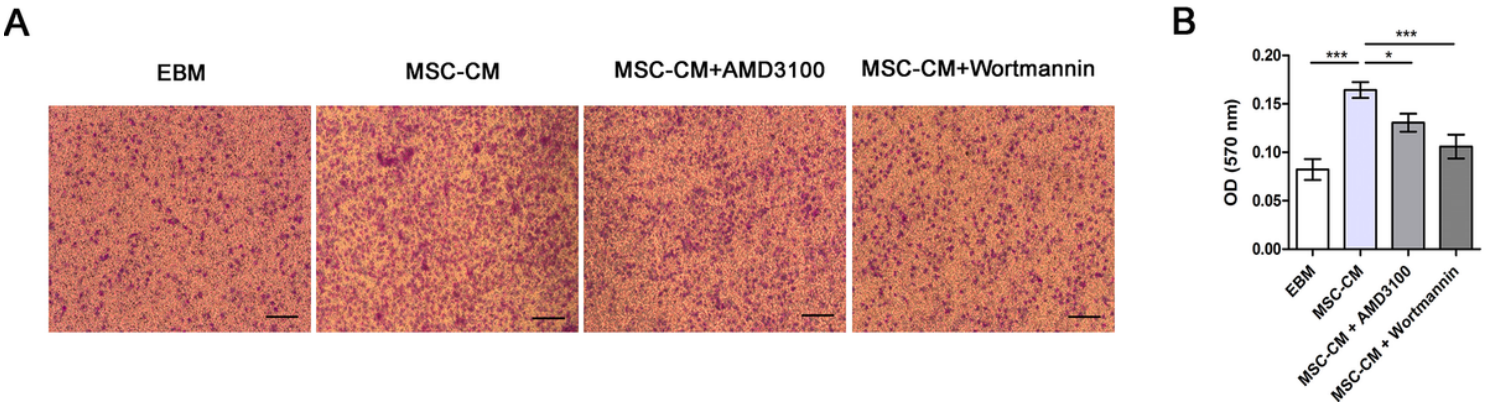

Figure 4

Representative photographs of EPC migration. (A) EPCs that migrated to the subsurface of the inserts were stained with crystal violet in the EBM, MSC, MSC + AMD3100, and MSC + wortmannin groups (n = 3). Scale bar, 200 μm. (B) Quantification analysis of migrating EPCs. Three independent trials were performed. *p < 0.05, ***p < 0.001.

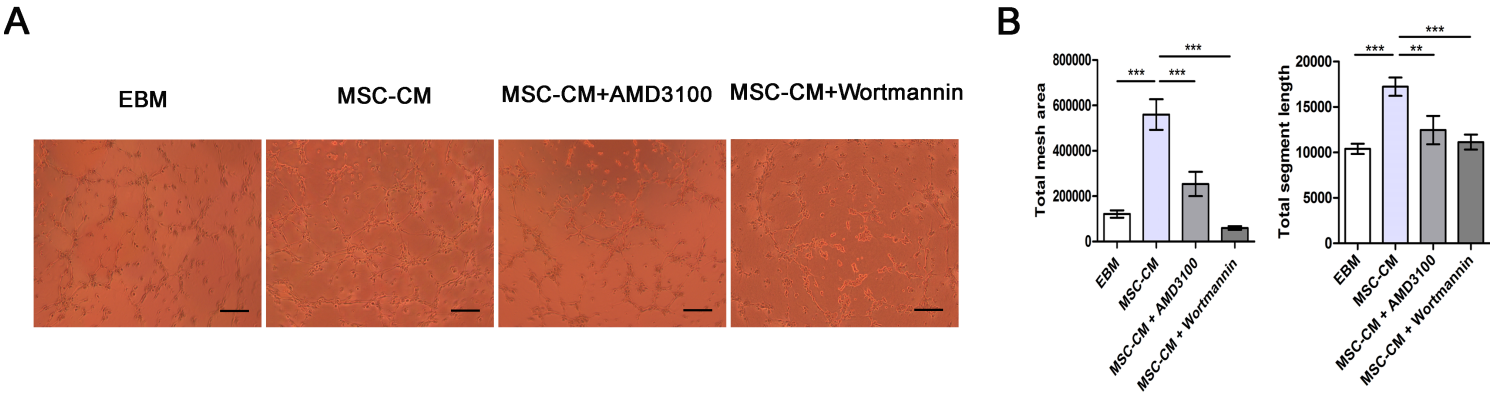

Figure 5

Representative photographs of EPC tubule formation. (A) Tube-like structures were formed by EPCs under the indicated conditions (n = 3). Scale bar, 200 μm. (B) Quantification of total mesh area and total segment length in the tube-like structure. The experiment was repeated thrice. **p < 0.01, ***p < 0.001.

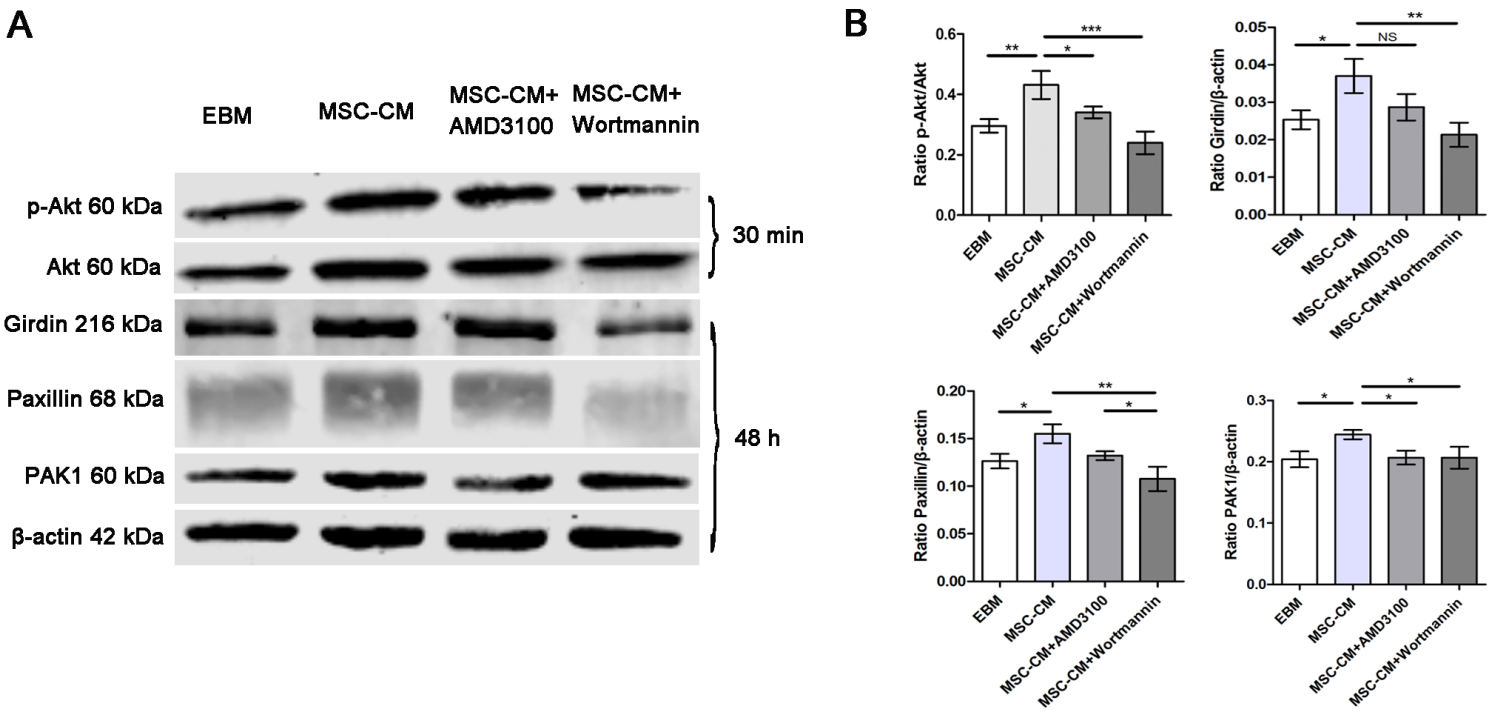

Figure 6

Role of the Akt pathway in MSC-secreted SDF-1 induction of EPC migration. (A) Expression of Akt protein and Akt phosphorylation levels in EPCs cultured for 30 min in the EBM, MSC-CM, MSC-CM + AMD3100, and MSC-CM + wortmannin groups. (B) Bar graphs show the ratio of the densitometry measurement of phosphor-Akt to that of β-actin and to that of Akt. Data were obtained from three independent experiments. *p < 0.05, **p < 0.01, ***p < 0.001, NS: no significance.